

Development of the stimulated Raman spectrum in single-mode silica fibers

R. H. Stolen and Clinton Lee*

AT&T Bell Laboratories, Holmdel, New Jersey 07733

R. K. Jain

Hughes Research Laboratories, Malibu, California 90265

The spectral development of stimulated Raman scattering in single-mode silica fibers was studied both experimentally and by computer modeling. The most striking feature that emerges is the rapid growth of a weak feature at 490 cm^{-1} at the expense of a broad band at 440 cm^{-1} as pump power increases. These experimental results are in good agreement with our numerical simulations, although neither experiments nor calculations show the spectral broadening of higher Stokes orders commonly observed with high pump powers and at infrared wavelengths. It is shown that, in general, spectral broadening from four-wave mixing should be important in the development of the stimulated Raman spectrum. However, the present experiments fall into a regime of relatively low pump powers at visible wavelengths in which four-wave mixing is negligible and the stimulated spectrum depends only on the shape of the Raman gain curve.

INTRODUCTION

Typical stimulated Raman spectra in silica fibers consist of a series of cascaded Stokes orders separated by frequency shifts of 440 cm^{-1} corresponding to the peak of the broad Raman band of fused silica. The spectral width of each successive Stokes order usually becomes broader until finally the output becomes a smooth continuum, although a continuum does not always form.¹ The spectrum of the first Stokes order in fused silica typically contains a sharp line at 490 cm^{-1} and a broad band at lower frequencies. The details of the spectrum seem to depend on the characteristics both of the fiber and of the exciting laser, although the exact mechanism is not well understood. In the limit where the pump linewidth is comparable with the Raman frequency, a continuum is formed directly.² Liquid-filled fibers, which have sharp Raman lines, can show behavior quite similar to that of glass fibers,^{2,3} which has led to speculation that self-phase modulation⁴ or four-photon mixing⁵ may be as important as the width and the shape of the Raman band in the development of the observed spectrum.

In this paper we investigate the development of the stimulated Raman spectrum in silica-core single-mode fibers as a function of distance and pump power both by experiment and by numerical simulation. Experiments were performed with a polarization-preserving fiber pumped by a frequency-doubled *Q*-switched Nd:YAG laser at 532 nm and an ordinary single-mode fiber pumped by a mode-locked argon laser at 514.5 nm. The computer model includes only the fused-silica Raman gain spectrum and neglects group-velocity dispersion and self-phase modulation or four-photon mixing.

We find good agreement between experiments and calculations for the first and second Stokes orders. The most striking feature seen in both experiments and calculations is

an extremely rapid relative growth of the sharp Raman peak at 490 cm^{-1} relative to the broad band at 440 cm^{-1} . It appears that for relatively low-power visible pump radiation the broad Raman gain spectrum is sufficient to describe the development of stimulated Raman scattering in a fiber. The qualitative picture is that the stimulated spectrum first builds up by amplification of the spontaneous Raman background. Then Raman amplification transfers energy within the stimulated band, which sharpens the long-wavelength edge of the spectrum. The subsequent development of the second Stokes spectrum is similar, although it is always somewhat broader than the first Stokes spectrum. The relative importance of Raman amplification and spontaneous scattering varies with fiber diameter, pump wavelength, and pump power, although fairly large variations in such parameters are required to effect significant changes in the condition for threshold power. This insensitivity to changes in parameters is in agreement with earlier analytical results.⁶

EXPERIMENTAL

Apparatus

Two different studies of the experimental development of the stimulated Raman spectrum were performed. Both experiments are illustrated schematically in Fig. 1.

In the first experiment, the source was a cw mode-locked argon-ion laser operated at 514.5 nm. The silica-core fiber was 100 m long, had a core diameter of $3.3\text{ }\mu\text{m}$ and a loss at 514.5 nm of 17 dB/km, and did not preserve linear polarization. The power in the fiber was varied by changing the drive current to the laser and was measured by means of a beam splitter internal to the laser. Measurement of the power out of the fiber showed the input coupling efficiency to be 70%. The pulse separation was 12 nsec. Accurate fiber measure-

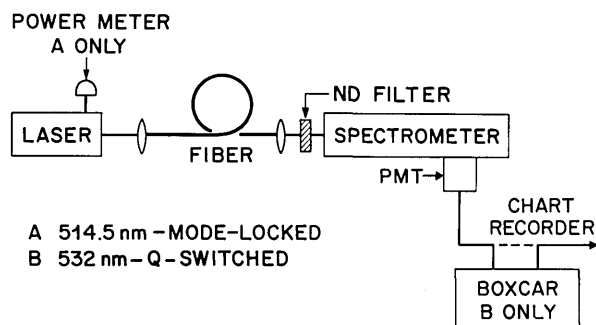


Fig. 1. Experimental arrangement for observing the development of the stimulated Raman spectrum. The output power of the mode-locked argon laser was measured with the laser's internal power meter. A boxcar amplifier was used to isolate the center of the output pulse of the Q-switched Nd:YAG laser.

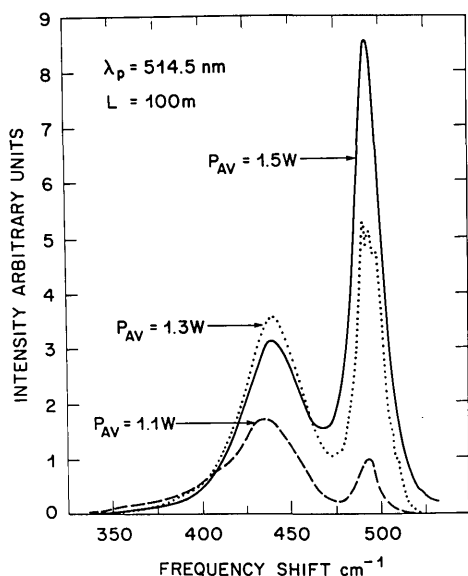


Fig. 2. Dependence of the first Stokes spectrum on the power of the mode-locked argon laser. The peak power in the fiber is approximately 12 times the average laser power.

ments using mode-locked lasers require some sort of isolation between the laser and the fiber. In the present experiments, no such isolator was used. Deliberate mistuning of the mode locker resulted in stable pulses of apparent pulse width ~ 700 psec over the entire range of drive currents used.

In the second experiment the source was a frequency-doubled, Q-switched Nd:YAG laser with an output wavelength of 532 nm. The output of this laser is a series of short pulses of the order of 100 psec separated by 4.6 nsec in an overall pulse envelope about 100 nsec long. A boxcar amplifier with a gate width of 20 nsec was used to isolate a section near the center of the pulse envelope where all the short pulses have approximately the same amplitude. The actual peak power coupled into the fiber was estimated to be of the order of 100 W. The fiber was a 173-m polarization-preserving fiber with a 4.0- μm -diameter silica core and a loss at 532 nm of 30 dB/km. The pump power was adjusted by varying the input coupling to the fiber.

Experimental Results

The first Stokes spectrum from the mode-locked pump at 514.5 nm is shown in Fig. 2 for three values of average laser

power. The peak power is approximately 12 times the average power as determined from the pulse width and coupling efficiency. The characteristic features in all three spectra are the broad peak around 440 cm^{-1} and the sharp peak at 490 cm^{-1} . As the pump power is raised, the 440-cm^{-1} maximum saturates and then drops, while the 490-cm^{-1} peak continues to grow. In Fig. 3 the peak intensities of these two maxima are plotted as a function of average laser power. These results show that both of the bands grow initially with energy supplied by the 514.5-nm pump and also, as discussed below, that energy is transferred within the Raman first Stokes band from the 440-cm^{-1} band to the 490-cm^{-1} peak.

The second experiment, with the Q-switched Nd:YAG laser, showed similar results, which are shown in Fig. 4. As the power was increased, the 490-cm^{-1} peak grew at a much faster rate than the 440-cm^{-1} maximum until the first Stokes band began to act as a pump for second Stokes output. The second Stokes band shows not the strong two-peak behavior of the first Stokes band but only a shift of the maximum within the band. The structure seen in the second Stokes spectrum of

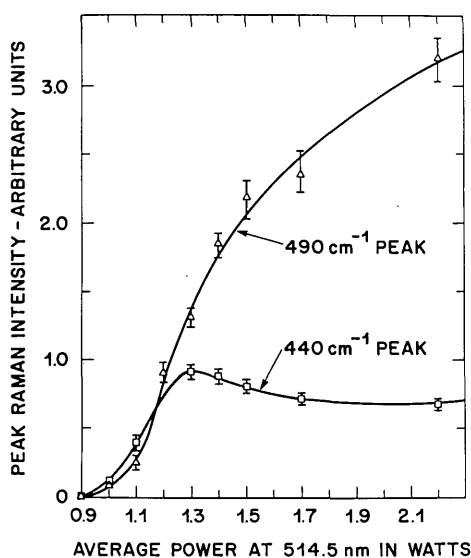


Fig. 3. Intensities of the 440- and 490-cm^{-1} Raman peaks as a function of mode-locked argon laser power. Peak power in the fiber is about 12 times the average laser power.

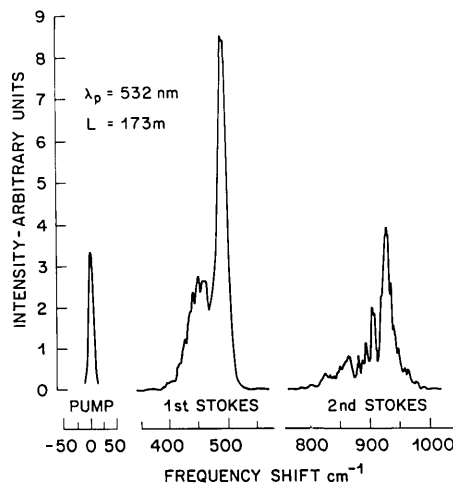


Fig. 4. First and second Stokes spectra pumped by the Q-switched Nd:YAG laser.

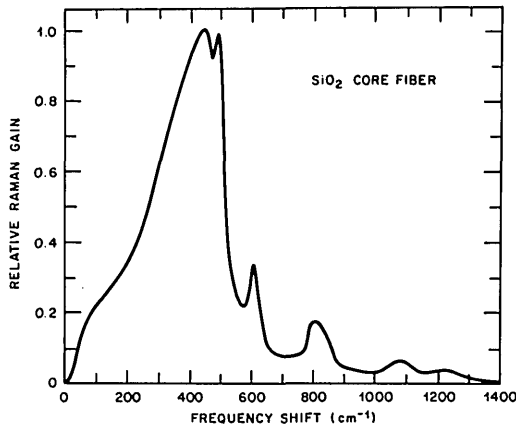


Fig. 5. Raman gain curve of a silica-core single-mode fiber. This curve is normalized to 1.0 at 440 cm^{-1} . The peak gain at 440 cm^{-1} for a pump wavelength of 532 nm is $1.86 \times 10^{-11} \text{ cm/W}$ and varies with pump wavelength as $1/\lambda_p$.⁸

Fig. 4 appears to be noise since it is quite different on every scan. These spectra have been corrected for the spectral response of the spectrometer and the photomultiplier.

At higher pump powers, about eight distinct Stokes orders were seen. Other fibers used with the same laser showed continuum generation after a few Stokes orders. On the other hand, 26 discrete Stokes orders were generated in a 400-m fiber with a 4.5- μm core diameter.

Raman Gain Curve

The Raman gain curve of fused silica, which was used for the calculations, is shown in Fig. 5. The gain curve is the spontaneous Raman spectrum divided by the thermal-population factor $[n(\Omega, T) + 1]$. The spectrum was obtained from the 173-m silica-core borosilicate-clad polarization-preserving single-mode fiber by using an exciting line at 441.6 nm from a He-Cd laser. Correction was made for instrumental response by calibrating the system with a lamp of known spectral output. No correction was made for the frequency dependence of the fiber loss or for the ω^4 factor in the spontaneous Raman cross section. The stimulated Raman spectrum is dominated by the region near the maximum, so these slowly varying corrections are relatively unimportant. The primary difference between spectra of different fused silica samples is found in the intensity of the sharp maxima at 490 and 604 cm^{-1} .⁷ The absolute gain at the broad maximum is known from earlier measurements.⁸

CALCULATED SPECTRUM

Procedure for Calculating the Amplification

In the calculations, the gain spectrum is divided into discrete frequencies 5 cm^{-1} apart. If we examine one frequency Ω_i of power S_i , the power gained from the pump power P over an incremental length Δl is $G(\Omega_i)S_i\Delta l P/A$, where Ω represents the shift from the pump frequency. The gain $G(\Omega_i)$ is obtained from Fig. 5, and A is an effective core area obtained from an integral over the mode field.⁸ Power at frequencies Ω_j less than Ω_i can also act to amplify the line at Ω_i with gain coefficients $G(\Omega_i - \Omega_j)$. In turn, Ω_i acts as a pump for frequency shifts Ω_k higher than Ω_i , again with gain coefficients determined by the frequency separation. The net power gain

or loss at Ω_i over a short length Δl at distance l along the fiber is then given by

$$dS_i(l) = g(\Omega_i)PS_i\Delta l + \sum_{j=1}^i g(\Omega_i - \Omega_j)S_jS_i\Delta l - \sum_{k=i+1}^N g(\Omega_k - \Omega_i)S_kS_i\Delta l, \quad (1)$$

where $g(\Omega) = G(\Omega)/A$. $G(\Omega)$ varies as λ_p^{-1} with pump wavelength. In like manner, the change in power is calculated at all frequencies including that of the pump. These are added or subtracted from the powers at the beginning of the interval Δl to give the spectrum at point l along the fiber.

Inclusion of Spontaneous Emission

The actual spectrum builds up not from an injected uniform background but rather from spontaneous emission along the fiber. From measurements of the Raman cross section of fused silica^{8,9} we can develop an approximate expression for the spontaneous Raman power (in watts) guided in the fiber:

$$dS_i(\text{spont}) = \frac{1.5 \times 10^{-27}}{\lambda^4} PG(\Omega_i)f\pi(\text{N.A.})^2\Delta\bar{\nu}\Delta l, \quad (2)$$

where $G(\Omega)$ is the gain curve from Fig. 5 and varies with pump wavelength as λ_p^{-1} , $\Delta\bar{\nu}$ is the frequency interval in units of inverse centimeters, P is the pump power, Δl is the incremental fiber length, and $f\pi(\text{N.A.})^2$ is the fraction of light scattered into 1 sr captured by the guide. In a highly multi-mode fiber all the light emitted within a solid angle given by the fiber's numerical aperture (N.A.) is guided so the factor $f = 1.0$. The numerical aperture is defined as $\sqrt{2n\Delta n}$, where Δn is the core-cladding-index difference. The solid angle and the Raman cross section contained in Eq. (2) are measured outside the sample. In single-mode fibers, f can vary between 0.2 and 0.7, depending on wavelength and fiber parameters.¹⁰ For convenience we choose a value of $f = 1/2$.

Equation (2) gives only the spontaneous Raman power scattered from the pump, but there will also be spontaneous Raman scattering from Ω_j to Ω_i and from Ω_i to Ω_k of Eq. (1). Spontaneous Raman scattering is then included in Eq. (1) by replacing S_i with $S_i + R$, where

$$R = \frac{1.5 \times 10^{-27}}{\lambda^4} \frac{\pi}{2} (\text{N.A.})^2 \Delta\bar{\nu} \frac{A}{G_m}. \quad (3)$$

In Eq. (3), G_m is the peak Raman gain, and we choose here a typical core-cladding-index difference $\Delta n = 0.005$, which gives $\text{N.A.} = 0.121$. For a wavelength of 532 nm and an effective area $A = 10^{-7} \text{ cm}^2$ (which corresponds to a core diameter of 3.75 μm), $R = 1.15 \times 10^{-7}$.

In the following calculations we examine the development of the spectrum for a pump wavelength of 0.532 μm and use a frequency interval of 5 cm^{-1} . We also neglect the differences in the spectrum introduced by the thermal occupation of the phonon states.

Calculated Continuous-Wave Spectra

To examine the evolution of the first and second Stokes spectra we choose a 50-m length and the core size and N.A. given in the previous subsection. The step size Δl was 2.5 cm. The conversion of pump power to first Stokes power and first Stokes to second Stokes power is seen in Fig. 6, where the total

power in each order is plotted as a function of pump power. In the calculation, the power in the Stokes lines adds up to the initial pump power as a consequence of the neglect of fiber absorption and the approximation that $\nu_p \approx \nu_{s1} \approx \nu_{s2}$.

The evolution of the first Stokes spectrum is shown in Fig. 7 for cw pump powers of 15, 20, 25, and 30 W. Note the change of scale for the 15-W spectrum, for which the conversion from the pump is small. As can be seen from Figs. 6 and 7, for pump powers above 20 W all the pump power is converted into first Stokes radiation, which in turn flows to the 490-cm⁻¹ line. The buildup of the 490-cm⁻¹ line is limited by the onset of second Stokes emission at a pump power around 35 W. Hereafter, the second Stokes band grows at the expense of the first Stokes band. The second Stokes band is pumped by the whole first Stokes band, not just by the strong 490-cm⁻¹ line.

Calculated Pulsed Spectra

The evolution of the spectra of the higher Stokes orders was investigated by carrying the computations out to the fifth

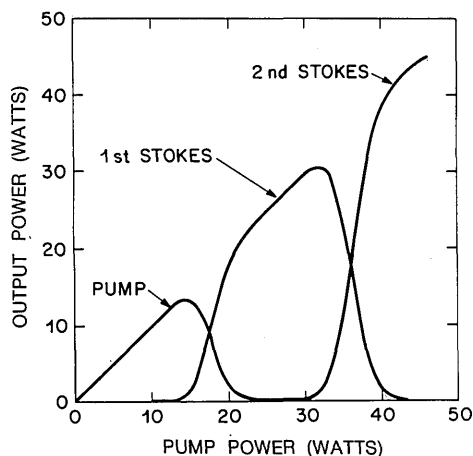


Fig. 6. Calculated output power as a function of input cw pump power. The pump wavelength is 532 nm, the fiber length is 50 m, and the effective core area is 10^{-7} cm².

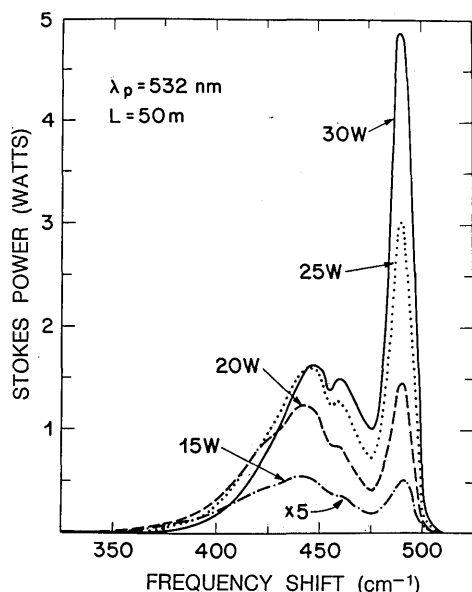


Fig. 7. Calculated first Stokes spectrum as a function of cw pump power. The pump and fiber parameters are the same as for Fig. 6.

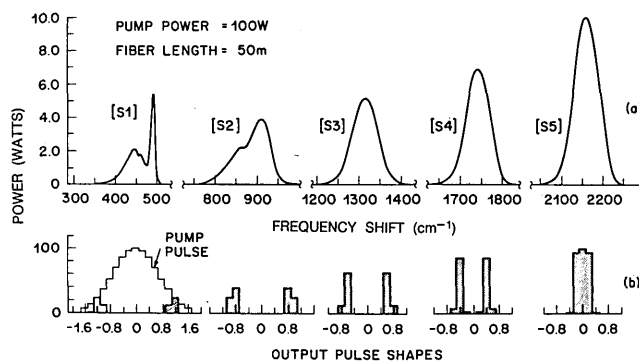


Fig. 8. Evolution of the stimulated Raman spectrum to the fifth Stokes order calculated for a Gaussian pump pulse depicted by the solid line in (b). The fiber length is 50 m, and the peak pump power is 100 W at 532 nm. The shaded areas for the various Stokes orders are the final computed pulse shapes at the fiber output.

Stokes order, as shown in Fig. 8(a). Rather than for a cw wave, the spectrum was calculated for a Gaussian input pump pulse. Shown in Fig. 8(b) is the output pulse shape at each of the Stokes orders. The peak pump power was 100 W at 532 nm, and the fiber was again 50 m long, but the step size was reduced to 1 cm. Each successive Stokes order is pumped by the center of the preceding Stokes pulse. This sequential depletion of the center of the pulse has been seen in continuum generation.² It was assumed that there was no group-velocity dispersion to cause walk-off between the pump and various Stokes orders. The division of pump energy into various Stokes orders depends on instantaneous pump power consistent with the behavior illustrated in Fig. 6. The evolution of the first Stokes spectrum as a function of power was also calculated for the Gaussian pulse, but the early part of the conversion from the pump is dominated by the pulse maximum, and the calculated pulsed spectrum differs little from the calculated cw spectrum.

DISCUSSION

Comparison of the calculated and measured spectra as a function of power shows that the basic experimental spectral features are reproduced in the cw calculations. The primary qualitative difference between experiment and calculations is that the experimental 490-cm⁻¹ peak starts out somewhat weaker than the 440-cm⁻¹ peak, while the two peaks start out with roughly comparable intensity in the calculations. This difference is probably because of a slightly lower 490-cm⁻¹ intensity in the Raman gain spectrum of the fiber used with the mode-locked argon laser. Although we do not have a Raman spectrum for this fiber, it has a high OH content, and it is known that the presence of OH reduces the peak intensity of both the 490- and 604-cm⁻¹ Raman lines.⁷

The peak pump powers for the measurements of Fig. 2 and the calculations of Fig. 7 are in fairly close agreement. The experimental powers should, however, have been about a factor of 2 higher because a polarization-preserving fiber was not used but the calculations assumed linear polarization. Raman gain is typically reduced by a factor of 2 when polarization is not preserved.¹¹ This particular fiber was slightly birefringent and, with sufficient care, would preserve linear polarization. It is possible that the polarization was substantially linear during the measurements. It is also possible

that the pump pulse was somewhat shorter than 700 psec because of inaccuracies arising from the slow response of the detector. More-recent measurements of pulse length from similar lasers using faster detectors showed that 400 psec is a more-typical pulse width when the mode locker is mis-tuned.

The variation of calculated pump and Stokes powers as plotted in Fig. 6 permits comparison of the present results with previous predictions of stimulated Raman threshold powers.^{6,12} In the earlier work, an expression for the stimulated Raman threshold was developed by assuming a Lorentzian gain profile and defining a critical power for which the Stokes and pump powers were equal⁶:

$$\gamma^{3/2}e^{-\gamma} = \frac{\sqrt{\pi}}{2} h\nu_s G_0 \frac{\Delta\nu_{1/2}}{A} L_{\text{eff}},$$

$$\gamma = G_0 \frac{P_c(0)}{A} L_{\text{eff}}, \quad (4)$$

where P_c is the critical power as measured as the fiber input, A is the effective core area, G_0 is the maximum Raman gain coefficient, ν_s is the Stokes frequency, and h is Planck's constant. L_{eff} is an effective fiber length that becomes the actual fiber length in the limit of negligible loss. The bandwidth $\Delta\nu_{1/2}$ is the FWHM of the assumed Lorentzian-Raman gain curve. This expression was later shown to be valid even when pump depletion was included.¹²

If we ignore the fact that the actual gain curve bears little resemblance to a Lorentzian curve, we can use Eq. (4) to calculate a threshold power for a fiber with the parameters used in the computations. From Fig. 5, $\Delta\nu_{1/2}/c = 250 \text{ cm}^{-1}$, which gives $\gamma = 17.25$ and $P_c = 18.5 \text{ W}$. This power can be compared with a critical power of 17.5 W from Fig. 6. In Eq. (4), $\Delta\nu_{1/2}$ actually functions as a coefficient in an expansion of $G(\nu) \approx G_0 [1 - 4(\nu - \nu_0)^2/\Delta\nu_{1/2}^2]$. Given the facts that the actual gain curve differs from a Lorentzian and that no simple expansion is possible near the actual gain maximum, the agreement between the computations and the analytic threshold condition is extremely good. By choosing $\Delta\nu_{1/2}/c = 600 \text{ cm}^{-1}$, one obtains exact agreement with $\gamma = 16.3$.

The good agreement between the experimental development of the stimulated first Stokes Raman spectrum and the present calculations, which neglect self-phase modulation or four-wave mixing, suggests that only the broad Raman gain curve is necessary to explain the evolution of the Raman spectrum. As the calculations are carried to higher orders, however, no evidence of broadening is found. This lack of broadening is contrary to results from most experiments, particularly those using pump lasers at 1.06 μm .

An explanation for the presence or lack of spectral broadening may lie in the differences to be expected in four-wave mixing at low or high powers or between the visible and the near infrared. At small frequency separations, four-wave mixing and self-phase modulation are just different ways of looking at the same process.¹³ In general, four-wave mixing will broaden the spectrum over a bandwidth $\Delta\nu_B$, which varies inversely with length. For sequential stimulated Raman scattering the relevant length would be the length over which a given Stokes order is strong. This length becomes shorter for higher pump powers. Thus at low pump powers the conversion distance is long, and four-wave mixing occurs over

a bandwidth that is negligible compared with the total Raman spectrum. As the pump power is raised, the conversion length decreases, and the additional broadening from four-wave mixing starts to make a significant contribution to the spectrum.

The relation between the length and the maximum frequency separation is given by the coherence length for a frequency separation Ω (Refs. 5 and 14):

$$l_{\text{coh}} = [\lambda D(\lambda) \Omega^2]^{-1}. \quad (5)$$

Thus the bandwidth is small for the long conversion lengths associated with low pump powers. For example, in Fig. 6 a pump power of only 30 W leads to maximum first Stokes conversion in 50 m at $\lambda = 532 \text{ nm}$. In Eq. (5) λ is the wavelength in centimeters, Ω the frequency shift in inverse centimeters, and $D(\lambda)$ the group-velocity dispersion in dimensionless units.¹⁵ At 532 nm $D(\lambda)$ is 0.073, so a coherence length of 50 m corresponds to a frequency shift of 7.1 cm^{-1} . A contribution to the broadening of only 7.1 cm^{-1} would not be noticed. If the power is strong enough, however, that Raman first Stokes conversion takes place over only 1 m, the broadening will be about 50 cm^{-1} , which is large enough to alter the spectrum. The dispersion $D(\lambda)$ approaches zero near 1.3 μm , so broadening from four-wave mixing becomes more important for infrared wavelengths. The broadening will be almost a factor of 10 larger for a 1.06- μm pump wavelength than for a pump at 532 nm. It will thus be difficult to avoid the effects of four-wave mixing in stimulated Raman scattering pumped by an infrared laser.

In the present paper we have also neglected walk-off between the pump pulse and the generated Stokes pulses. In a 100-m fiber with a 532-nm pump, pump and Stokes pulses introduced together at the fiber input will separate by about 600 psec. In the experiment with the 514.5-nm mode-locked pulses the pump-pulse length was 700 psec, and such walk-off is probably not important. In the experiment with the YAG laser, however, the 100-nsec pulse was made up of pulses approximately 100 psec long, so pulse walk-off must be taking place. It is clear from the experimental results that walk-off does not modify the qualitative features of the spectrum, although one would expect conversion within the pulse to be emphasized with respect to conversion to or from another Stokes order.

CONCLUSION

There appears to be a regime of long fibers and relatively low pump powers at visible wavelengths in which the nonlinear spectrum can be described by stimulated Raman scattering alone. In this regime, Raman amplification not only transfers pump power to successively higher Stokes orders but also transfers energy to longer wavelengths within each Stokes order. It is particularly useful to have a regime in which some simplification is possible since the general problem of stimulated Raman-type spectra in fibers is quite complicated. A general treatment should include broadening from four-wave mixing and pulse walk-off resulting from group-velocity dispersion. The present work already suggests ways in which four-wave mixing and pulse walk-off will modify the spectral evolution, although more-accurate experiments will be necessary for these contributions to be understood.

* Present address, Department of Electrical Engineering, North Carolina State University, Raleigh, North Carolina 27650.

REFERENCES

1. R. H. Stolen, "Nonlinear properties of optical fibers", in *Optical Fiber Telecommunications*, S. E. Miller and A. G. Chynoweth, eds. (Academic, New York, 1979), Chap. 5; L. G. Cohen and Chinlon Lin, "A universal fiber-optic (UFO) measurement system based on a near-IR fiber Raman laser," *IEEE J. Quantum Electron.* **QE-14**, 855-859 (1978); V. S. Butylkin, V. V. Grigoryants, and V. I. Smirnov, "On the role of SRS in the transmission of intense laser light through silica-fiber light-guides," *Opt. Quantum Electron.* **11**, 141-146 (1979); G. Rosman, "High-order spectrum from stimulated Raman scattering in a silica-core fiber," *Opt. Quantum Electron.* **14**, 92-93 (1982); Gao Pei-juan, Nie Cao-jiang, Yang Tian-long, and Su Hai-zheng, "Stimulated Raman scattering up to 10 orders in an optical fiber," *Appl. Phys.* **24**, 303-306 (1981); F. R. Barbosa, "Quasi-stationary multiple stimulated Raman generation in the visible using optical fibers", *Appl. Opt.* **22**, 3854-3863 (1983).
2. Chinlon Lin and R. H. Stolen, "New nanosecond continuum for excited-state spectroscopy," *Appl. Phys. Lett.* **28**, 216-218 (1976).
3. E. P. Ippen, "Low power quasi-cw Raman oscillator," *Appl. Phys. Lett.* **16**, 303-305 (1970).
4. R. H. Stolen and Chinlon Lin, "Self-phase modulation in silica optical fibers," *Phys. Rev. A* **17**, 1448-1453 (1978).
5. K. O. Hill, D. C. Johnson, B. S. Kawasaki, and R. I. MacDonald, "Cw three-wave mixing in single-mode optical fibers," *J. Appl. Phys.* **49**, 5098-5106 (1978).
6. R. G. Smith, "Optical power handling capacity of low loss optical fibers as determined by stimulated Raman and Brillouin scattering," *Appl. Opt.* **11**, 2489-2494 (1972).
7. R. H. Stolen and G. E. Walrafen, "Water and its relation to broken bond defects in fused silica," *J. Chem. Phys.* **64**, 2623-2631 (1976).
8. R. H. Stolen and E. P. Ippen "Raman gain in glass optical waveguides," *Appl. Phys. Lett.* **22**, 276-278 (1973).
9. R. Hellwarth, J. Cherlow, and T-T. Yang, "Origin and frequency dependence of nonlinear optical susceptibilities of glasses," *Phys. Rev. B* **11**, 964-967 (1975).
10. P. O'Connor and J. Tauc, "Light scattering in optical waveguides," *Appl. Opt.* **17**, 3226-3231 (1978); B. Crosignani, P. DiPorto, and S. Solimeno, "Influence of guiding structures on spontaneous and stimulated emission: Raman scattering in optical fibers," *Phys. Rev. A* **21**, 594-598 (1980).
11. R. H. Stolen, "Polarization effects in fiber Raman and Brillouin lasers," *IEEE J. Quantum Electron.* **QE-15**, 1157-1160 (1979).
12. J. AuYeung and A. Yariv, "Spontaneous and stimulated Raman scattering in long low loss fibers," *IEEE J. Quantum Electron.* **QE-14**, 347-352 (1978).
13. J. Botineau and R. H. Stolen, "Effect of polarization on spectral broadening in optical fibers," *J. Opt. Soc. Am.* **72**, 1592-1596 (1982).
14. R. H. Stolen and J. E. Bjorkholm, "Parametric amplification and frequency conversion in optical fibers," *IEEE J. Quantum Electron.* **QE-18**, 1062-1072 (1982).
15. D. Gloge, "Weakly guiding fibers," *Appl. Opt.* **10**, 2252-2258 (1971).